Supporting Information

Towards Anisotropic Hybrid Materials: Directional Crystallization of Amphiphilic Polyoxazoline-based Triblock Terpolymers

Tobias Rudolph;[1,2] Matthias Hartlieb;[1,2] Moritz von der Lühe;[1,2] Sebastien Norsic;[3] Ulrich S. Schubert;[1,2,4] Christophe Boisson;[3] Franck D´Agosto;[3] Felix H. Schacher[1,2,*]

Affiliations

[1] Laboratory of Organic and Macromolecular Chemistry (IOMC), Friedrich Schiller University Jena, Humboldtstr. 10, 07743 Jena, Germany

E-mail: felix.schacher@uni-jena.de

[2] Jena Center for Soft Matter (JCSM), Friedrich Schiller University Jena, Philosophenweg 7, 07743 Jena, Germany

[3] Université de Lyon, Univ. Lyon 1, CPE Lyon, CNRS UMR 5265 Laboratoire de Chimie, Catalyse, Polymères et Procédés (C2P2), Equipe LCPP, Bat 308F, 43 Bd du 11 novembre 1918, F-69616 Villeurbanne, France

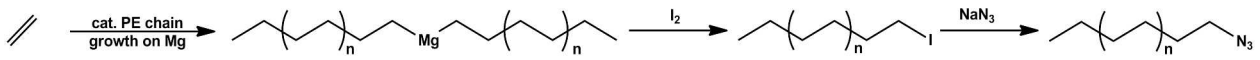

Scheme S1: Catalyzed polyethylene chain growth on Mg and subsequent conversion *via* iodide and sodium azide (NaN_3), leading to azide functionalized PE-N_3.

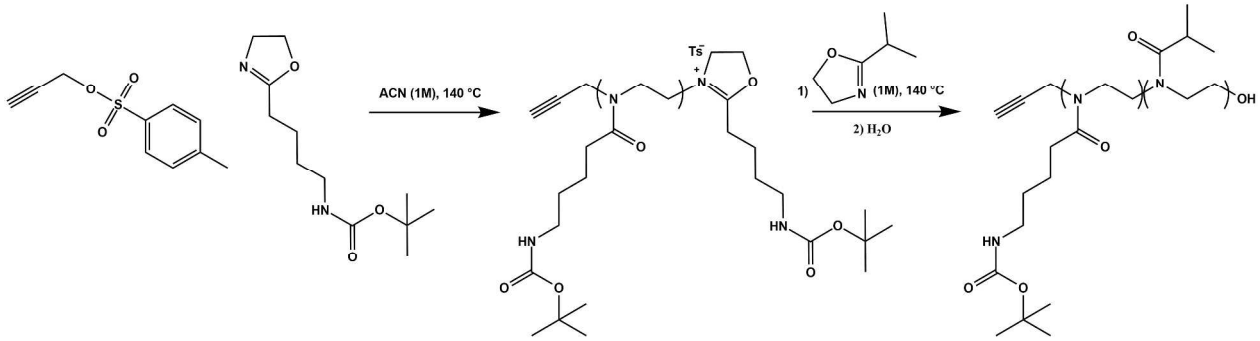

Scheme S2: Microwave-assisted CROP of alkyne functionalized diblock copolymers of poly-(2-(4-((*tert*-butoxycarbonyl)amino)butyl)-2-oxazoline)-*block*-poly(2-*iso*-propyl-2-oxazoline) (PBocAmOx-*b*-P*i*PrOx) initiated by propargyl *p*-toluenesulfonate.

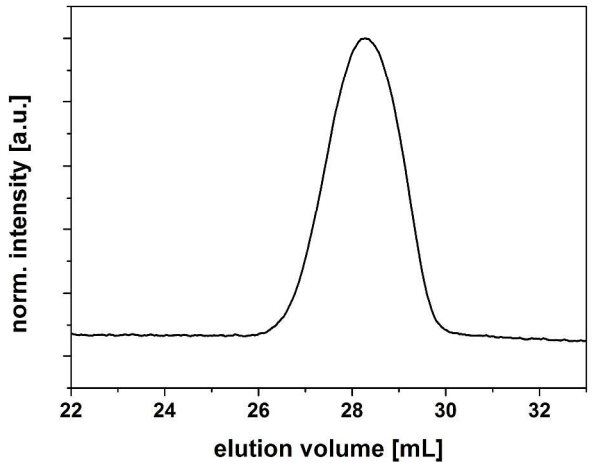

Figure S1: Molar mass distribution of PE_{36}-N_3 determined *via* high temperature SEC (column temperature: 150 °C; solvent: trichlorobenzene; M_n = 1290 g mol^{-1}; $Đ$ = 1.16).

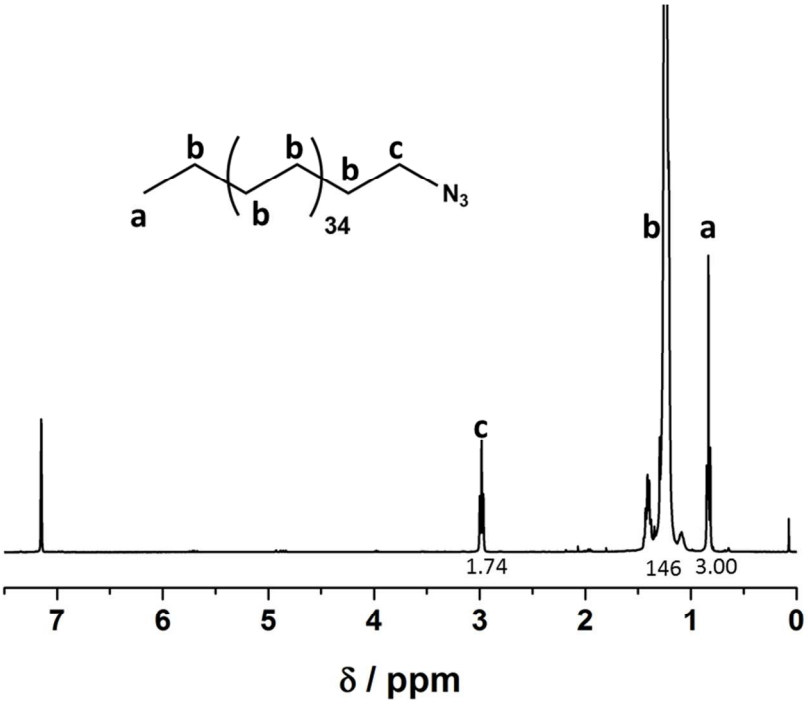

Figure S2: ^{1}H-NMR spectrum for PE_{36}-N_3; degree of azide-functionality of ≈ 87% (C_2Cl_4/C_6D_6 at 363K).

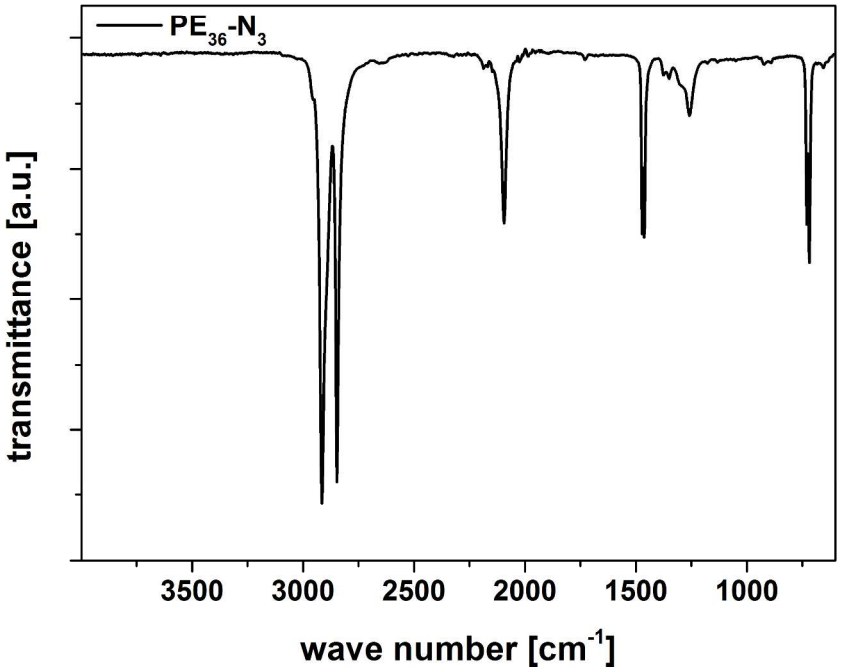

Figure S3: FT-IR spectrum for PE_{36}-N_3 and the characteristic peak for the azide at 2094 cm^{-1}.

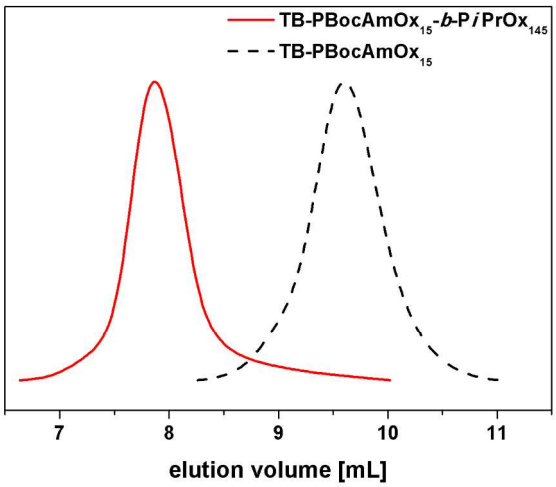

Figure S4: Comparison of SEC traces for TB-PBocAmOx$_{15}$ (dashed line) and TB-PBocAmOx$_{15}$-*b*-P*i*PrOx$_{145}$ (straight line) ($CHCl_3$-SEC).

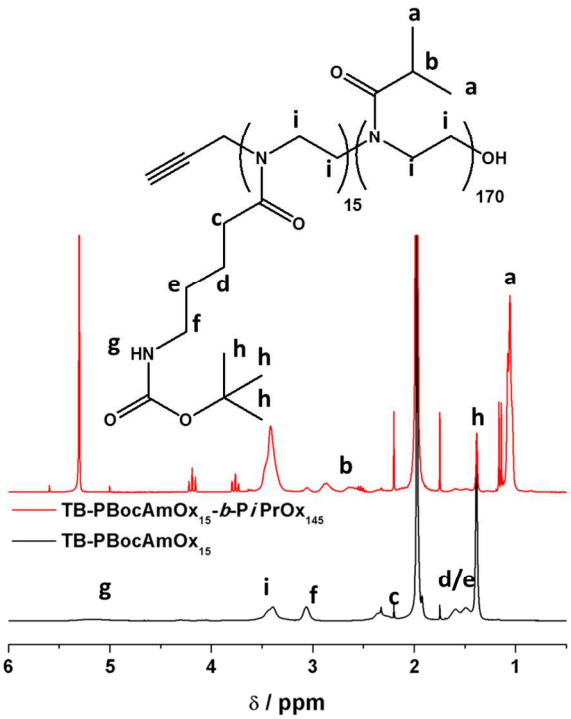

Figure S5: Comparison of NMR spectra for the block copolymerization of BocAmOx and *i*PrOx: TB-PBocAmOx$_{15}$ (black trace) and TB-PBocAmOx$_{15}$-*b*-P*i*PrOx$_{145}$ (red trace, 300 MHz; $CDCl_3$).

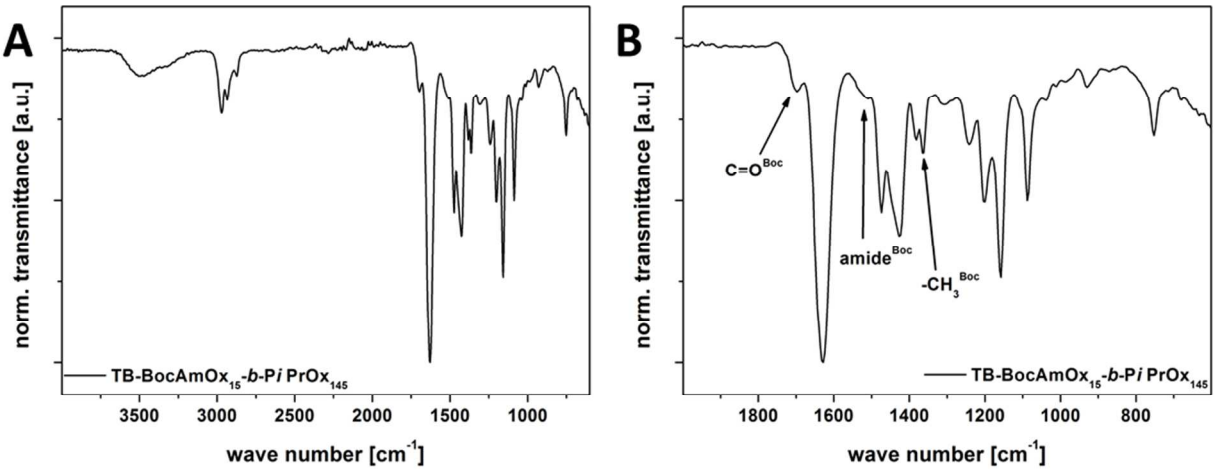

Figure S6: A) FT-IR spectrum for TB-PBocAmOx$_{15}$-*b*-P*i*PrOx$_{145}$ and an inset (B).

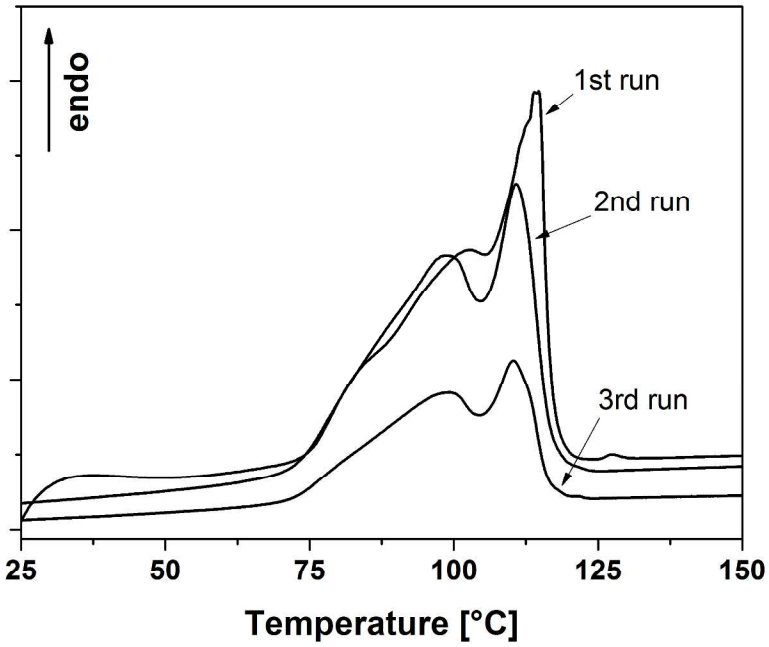

Figure S7: Comparison of DSC traces for PE$_{36}$-N$_3$: 1st run (20 K min^{-1}), 2nd run (20 K min^{-1}), and 3rd run (10 K min^{-1}).

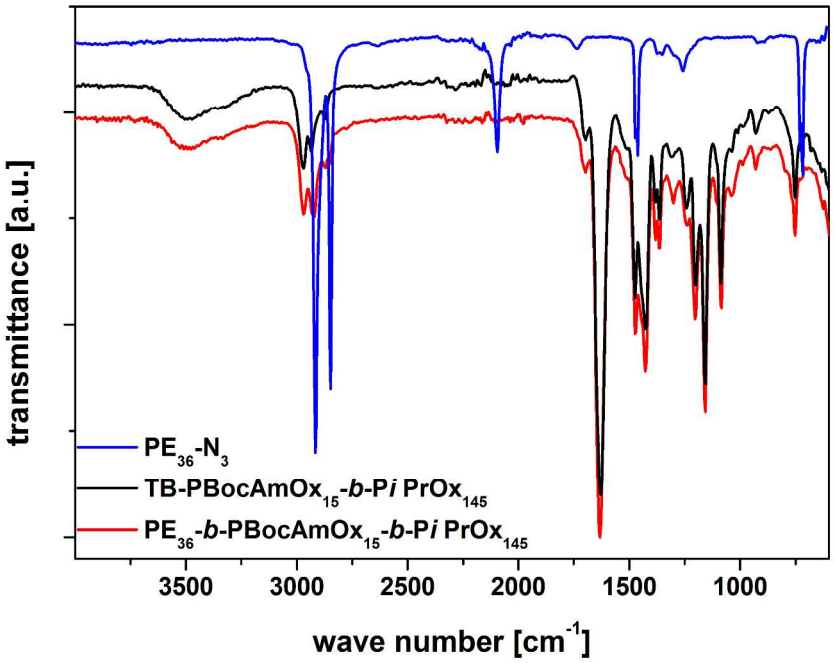

Figure S8: Comparison of FT-IR spectra for PE_{36}-N_3 (blue trace), $PBocAmOx_{15}$-*b*-P*i*$PrOx_{145}$ (black trace), PE_{36}-*b*-$PBocAmOx_{15}$-*b*-P*i*$PrOx_{145}$ (red trace).

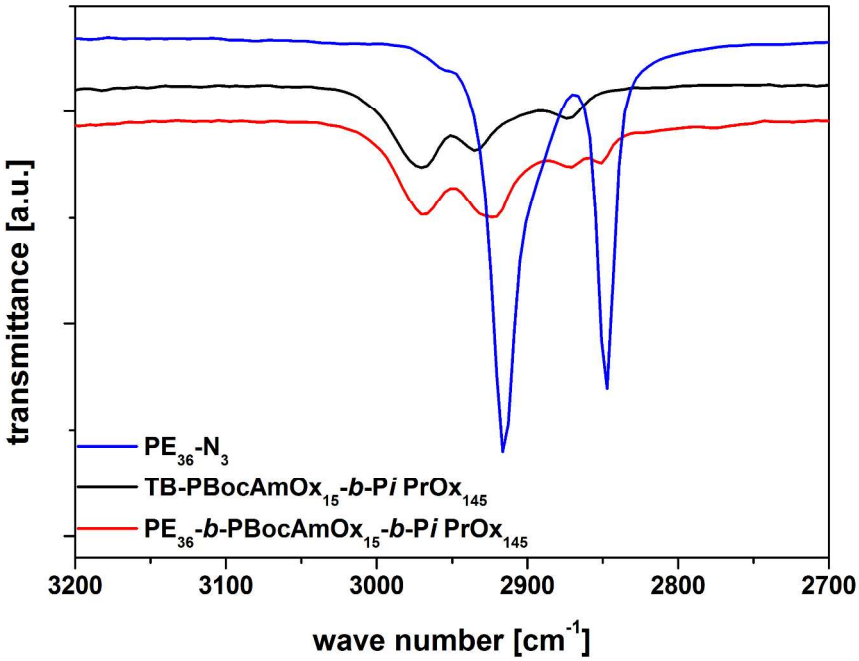

Figure S9: Comparison of FT-IR spectra in the range of 3200 to 2700 cm^{-1} for PE_{36}-N_3 (blue trace), $PBocAmOx_{15}$-*b*-P*i*$PrOx_{145}$ (black trace), PE_{36}-*b*-$PBocAmOx_{15}$-*b*-P*i*$PrOx_{145}$ (red trace).

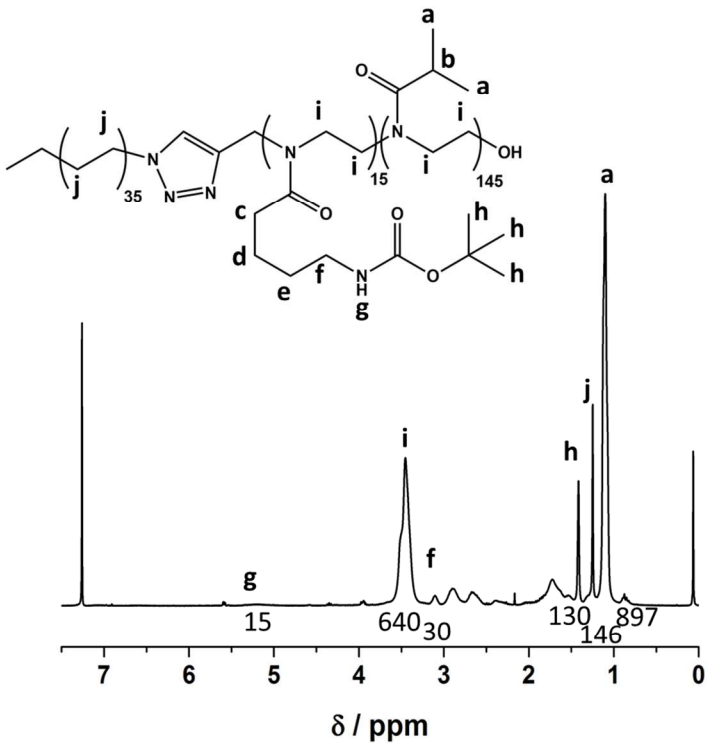

Figure S10: ^{1}H-NMR of PE$_{36}$-*b*-PBocAmOx$_{15}$-*b*-P*i*PrOx$_{145}$ and peak assignment and integration for characteristic signals (300MHz, CDCl$_3$).

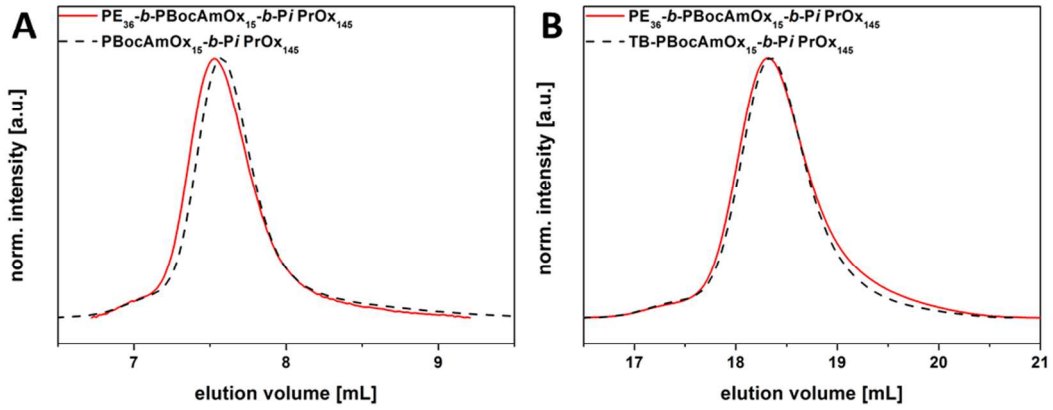

Figure S11: Comparison of SEC traces for PBocAmOx$_{15}$-*b*-P*i*PrOx$_{145}$ (black dashed line) and PE$_{36}$-*b*-PBocAmOx$_{15}$-*b*-P*i*PrOx$_{145}$ (red straight line) with different eluents: A) chloroform (CHCl$_3$), B) dimethylacetamide (DMAC).

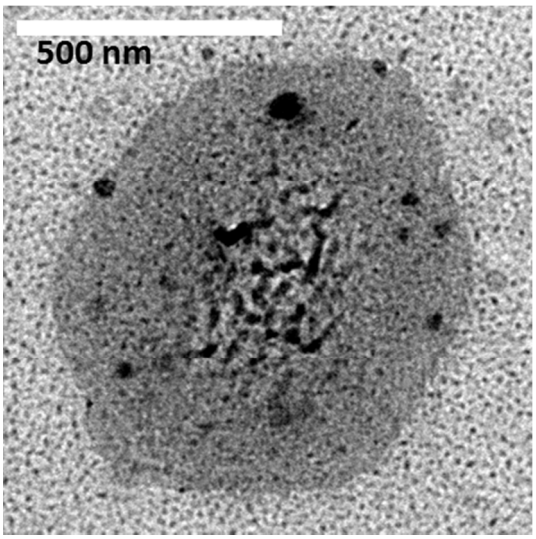

Figure S12: TEM micrograph for kite-like PE_{36}-N_3 aggregate obtained after heating in DMF to 120 °C and cooling to room temperature.

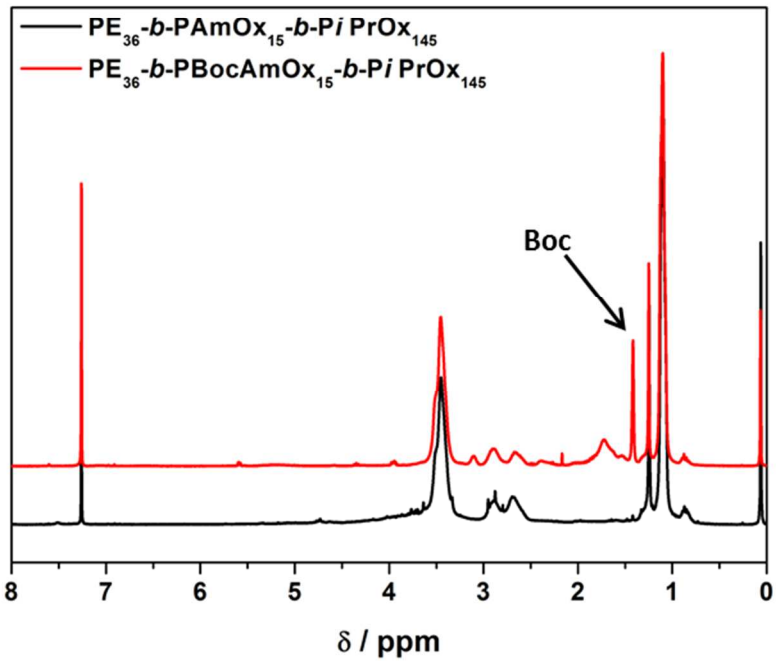

Figure S13: Comparison of NMR spectra before (red trace) and after (black trace) deprotection of PE_{36}-*b*-$PBocAmOx_{15}$-*b*-P*i*$PrOx_{145}$ (300MHz, $CDCl_3$).

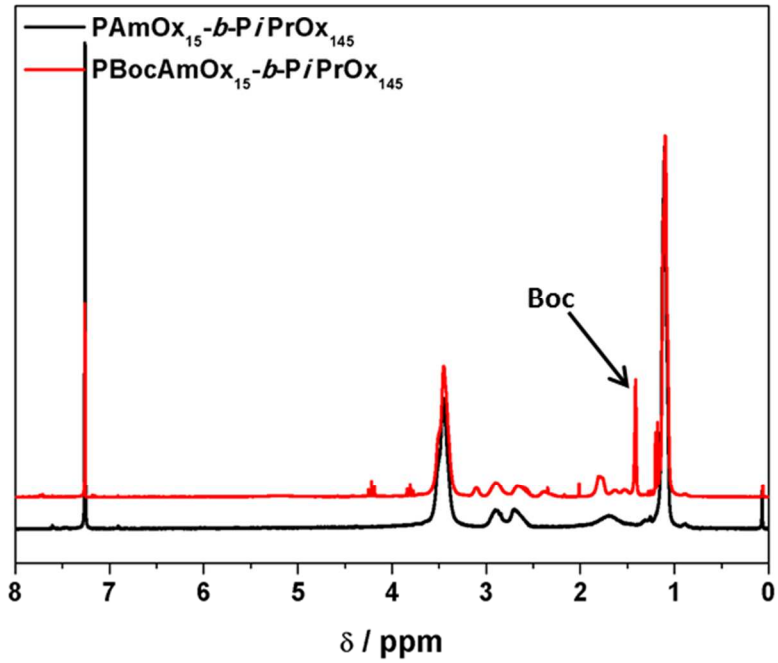

Figure S14: Comparison of ^{1}H-NMR spectra before (red trace) and after (black trace) deprotection of PBocAmOx$_{15}$-*b*-P*i*PrOx$_{145}$ (300 MHz, CDCl$_3$).

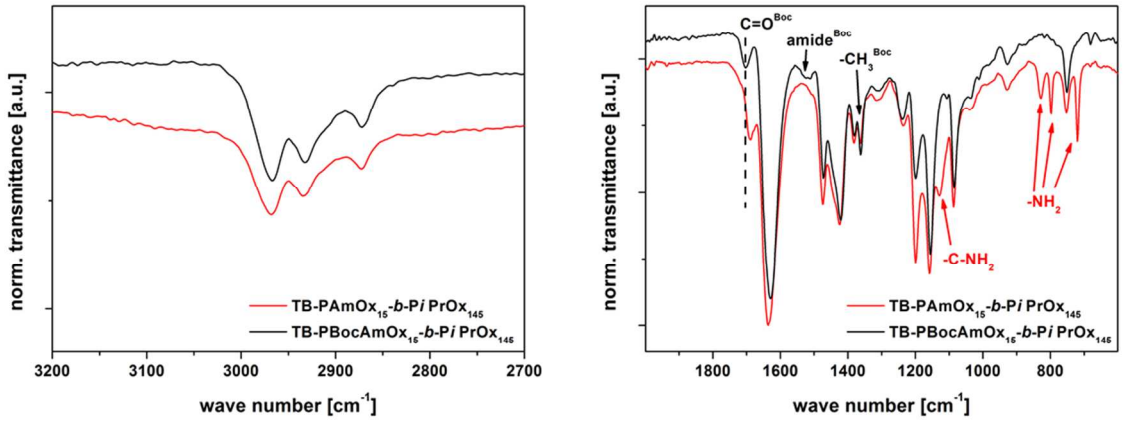

Figure S15: Comparison of FT-IR spectra before (black trace) and after (red trace) deprotection of PBocAmOx$_{15}$-*b*-P*i*PrOx$_{145}$.

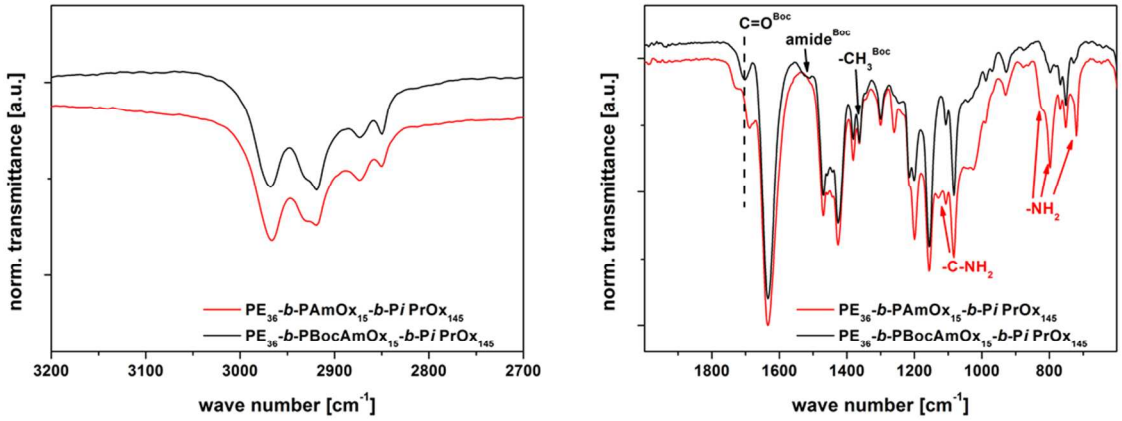

Figure S16: Comparison of FT-IR spectra before (black trace) and after (red trace) deprotection of PE_{36}-*b*-$PBocAmOx_{15}$-*b*-P*i*$PrOx_{145}$.

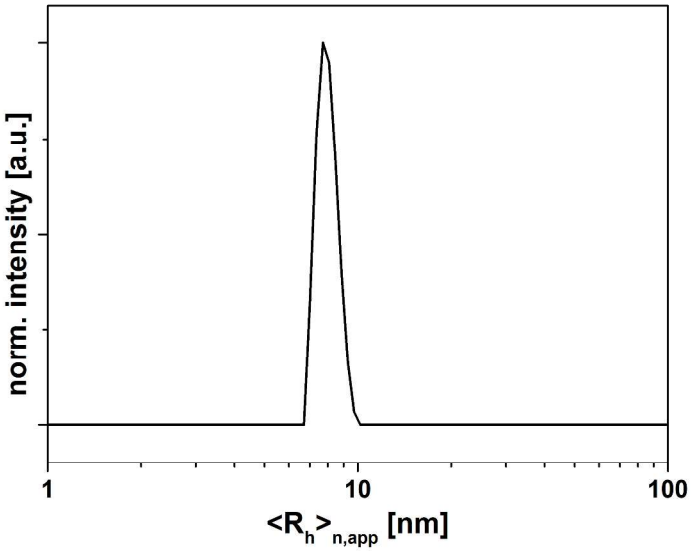

Figure S17: DLS CONTIN plot for PE_{36}-*b*-$PBocAmOx_{15}$-*b*-P*i*$PrOx_{145}$ after heating to 120 °C for 10 minutes and cooling to room temperature in DMF.

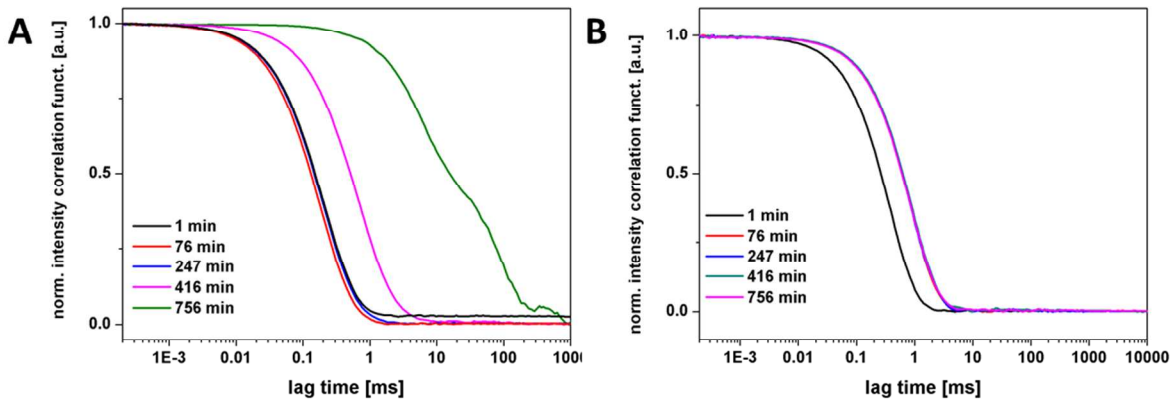

Figure S18: Time-dependent normalized intensity autocorrelation functions for PE$_{36}$-*b*-PAmOx$_{15}$-*b*-P*i*PrOx$_{145}$ (A) and PE$_{36}$-*b*-PBocAmOx$_{15}$-*b*-P*i*PrOx$_{145}$ (B) after: 1 (black line), 76 (red line), 247 (blue line), 416 (pink line) and 756 (green line) minutes.

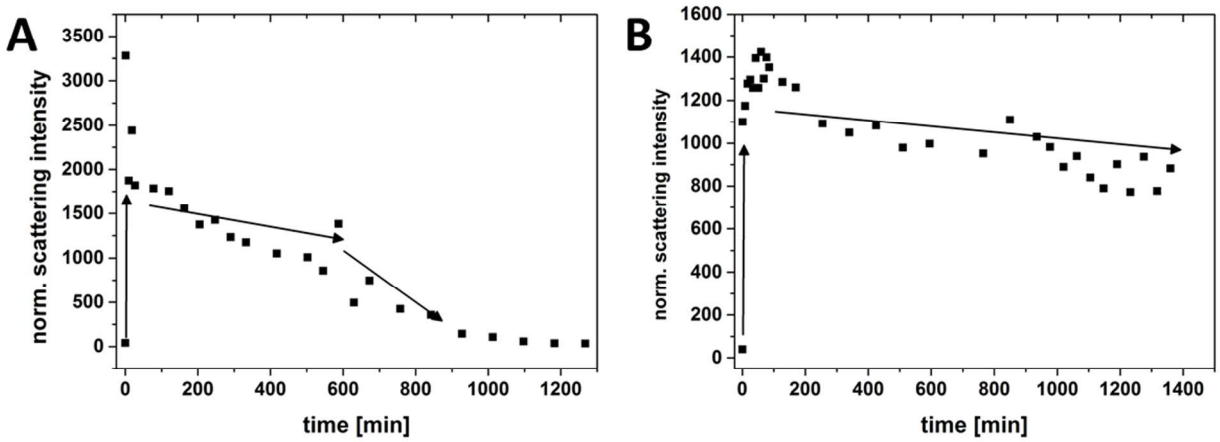

Figure S19: Normalized scattering intensity (black) over time annealed at 65 °C (0.1 mg mL^{-1}) for TB-PBocAmOx$_{15}$-*b*-P*i*PrOx$_{145}$ (A) and TB-PAmOx$_{15}$-*b*-P*i*PrOx$_{145}$ (B) diblock copolymers.

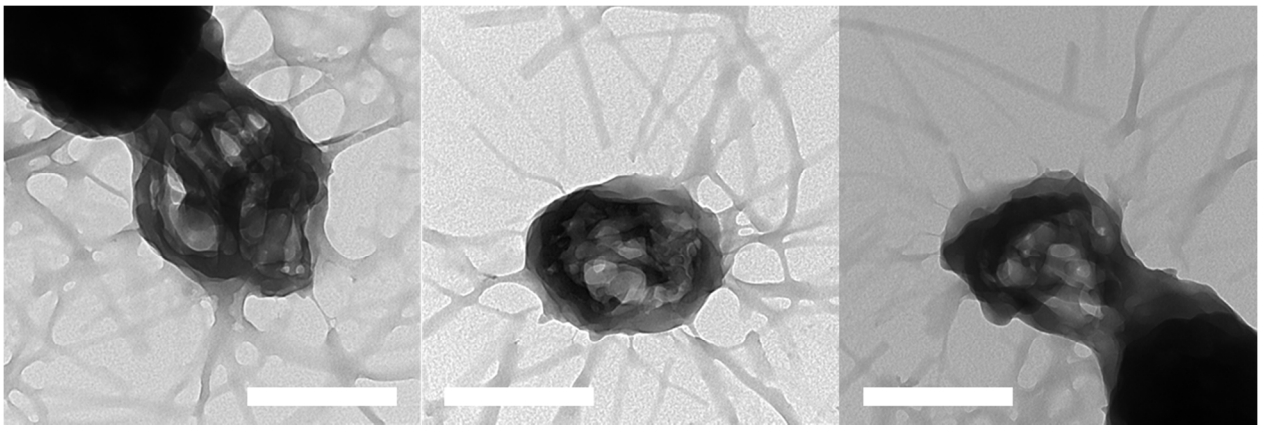

Figure S20: TEM micrographs for PBocAmOx$_{15}$-*b*-P*i*PrOx$_{145}$ after 24 hours at 65 °C in water (0.33 mg mL^{-1}).

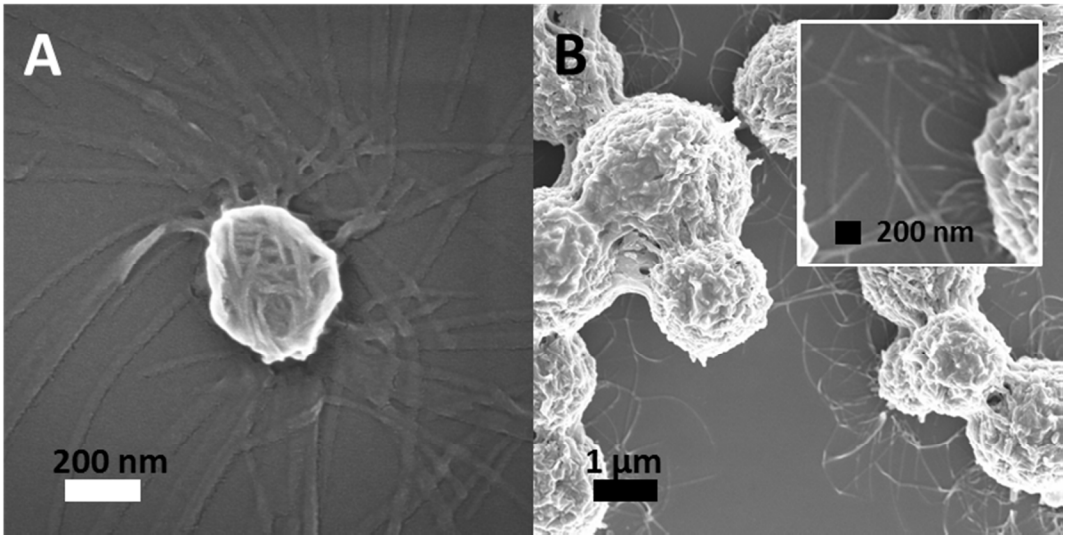

Figure S21: SEM micrographs for the diblock copolymers PAmOx$_{15}$-*b*-P*i*PrOx$_{145}$ (A) and PBocAmOx$_{15}$-*b*-P*i*PrOx$_{145}$ (B) after 24 hours at 65 °C in water (0.33 mg mL^{-1}), respectively.

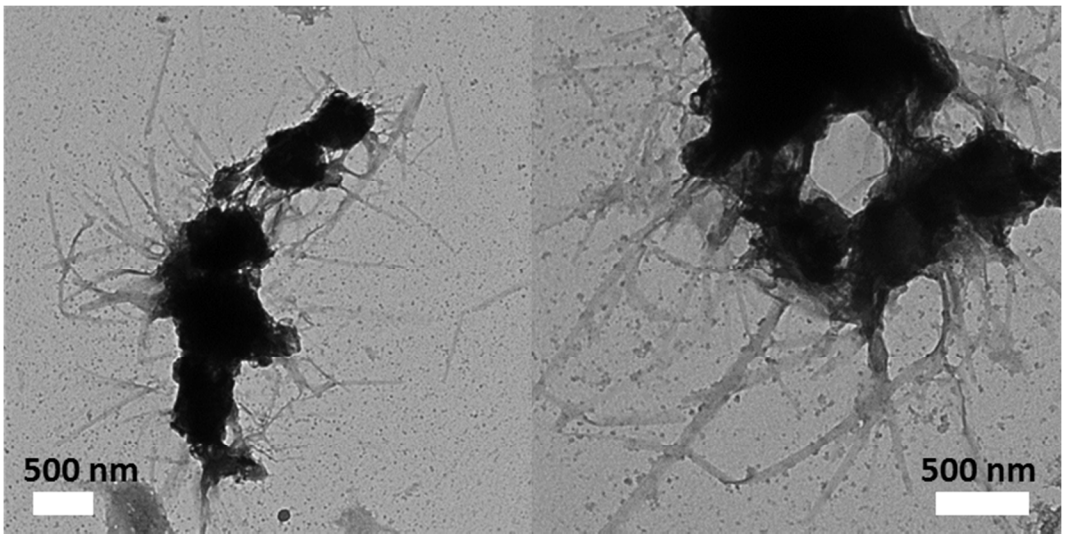

Figure S22: TEM micrographs for PE_{36}-*b*-$PAmOx_{15}$-*b*-P*i*$PrOx_{145}$ after 24 hours at 65 °C in water (0.33 mg mL^{-1}) at pH 12 (adjusted by NaOH).

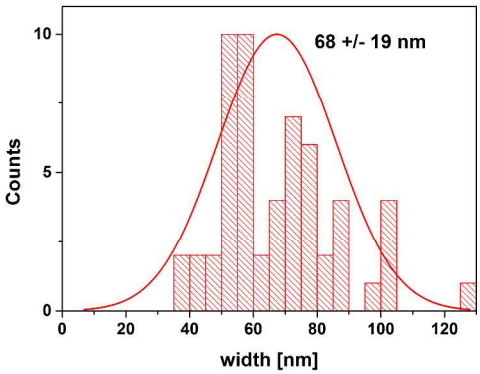

Figure S23: Histogram of width distribution determined for PE_{36}-*b*-$PAmOx_{15}$-*b*-P*i*$PrOx_{145}$ after directional crystallization of PiPrOx at pH 12 determined by grey-scale analysis from TEM micrographs (for 57 positions).

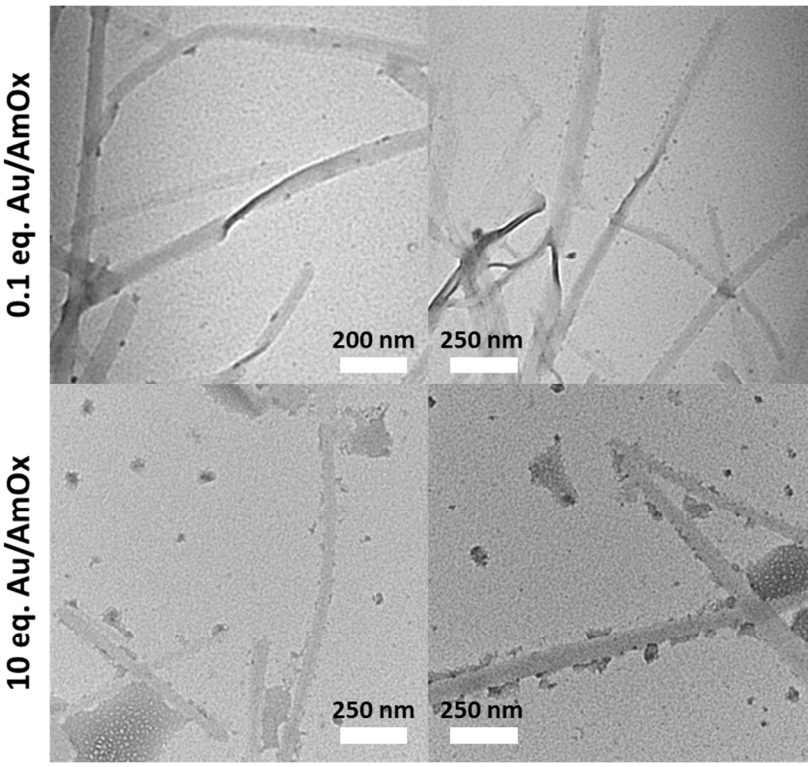

Figure S24: TEM micrographs for PE_{36}-*b*-$PAmOx_{15}$-*b*-P*i*$PrOx_{145}$ after 24 hours at 65 °C in water (0.33 mg mL^{-1}) and *in-situ* reduced $HAuCl_4$ with different equivalents of gold precursor to PAmOx: 0.1 eq. Au/AmOx (top micrographs) and 10 eq. Au/AmOx (bottom micrographs).

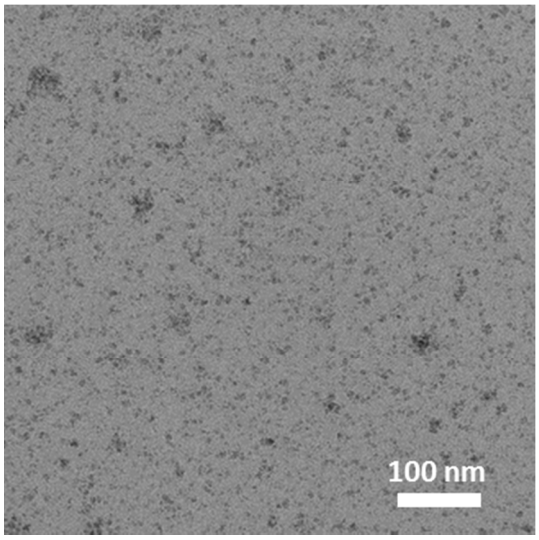

Figure S25: TEM micrograph for as-synthesized Fe_3O_4 -nanocrystals.

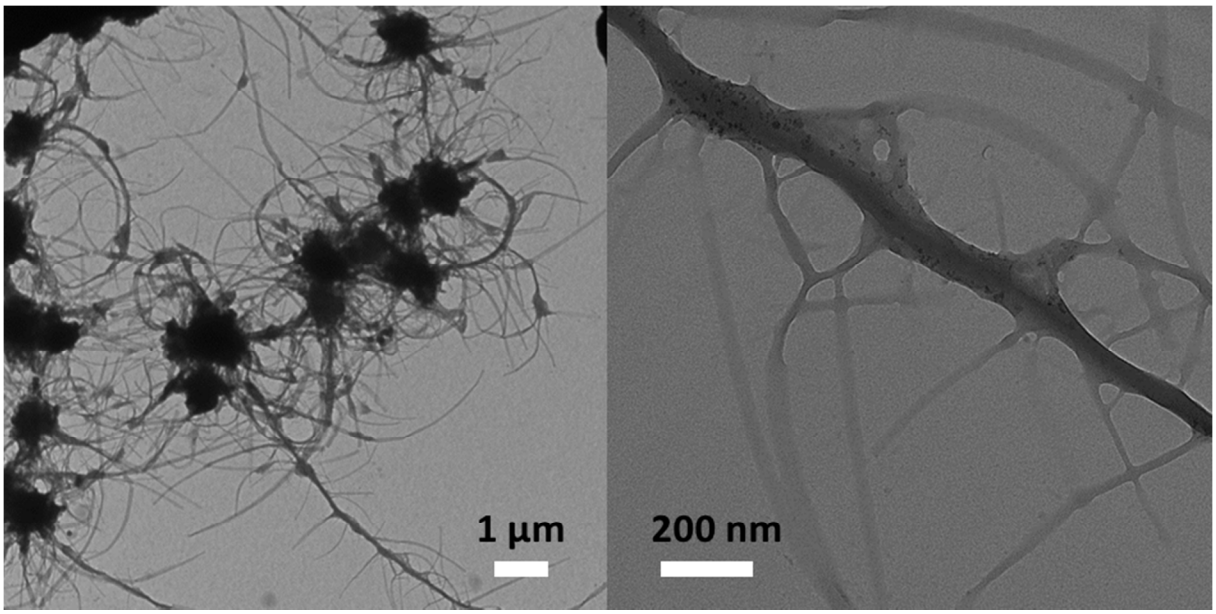

Figure S26: TEM micrographs for PE_{36}-*b*-$PAmOx_{15}$-*b*-P*i*$PrOx_{145}$ after 24 hours at 65 °C in water (0.33 mg mL^{-1}) and Fe_3O_4 nanocrystals.

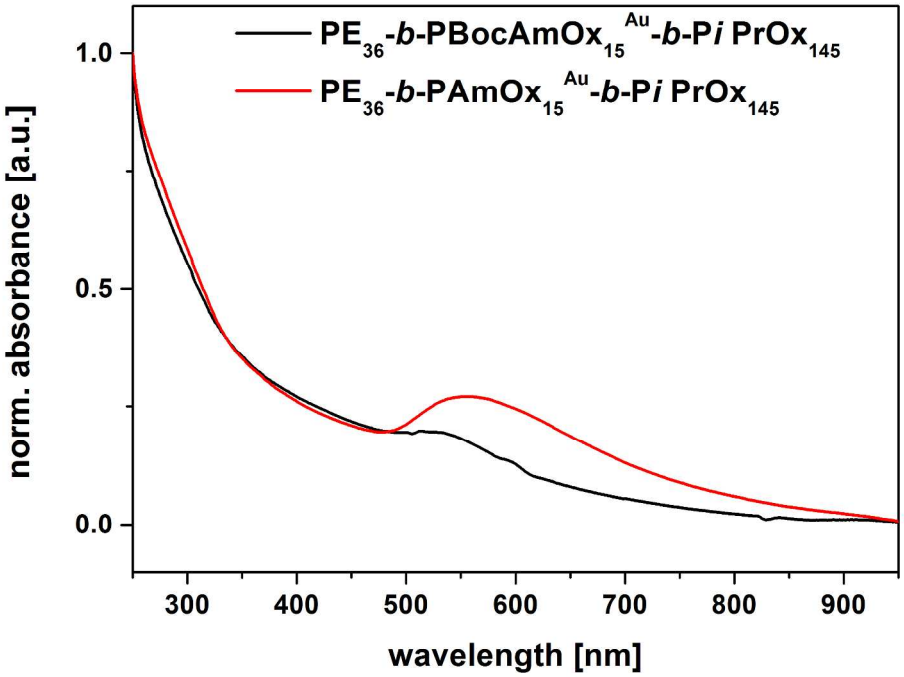

Figure S27: Comparison of UV-Vis spectra for PE_{36}-*b*-$PAmOx_{15}$-*b*-P*i*$PrOx_{145}$ (red trace) and PE_{36}-*b*-$PAmOx_{15}$-*b*-P*i*$PrOx_{145}$ (black trace) after reduction of $HAuCl_4$ (0.1 eq. Au/AmOx) in water.

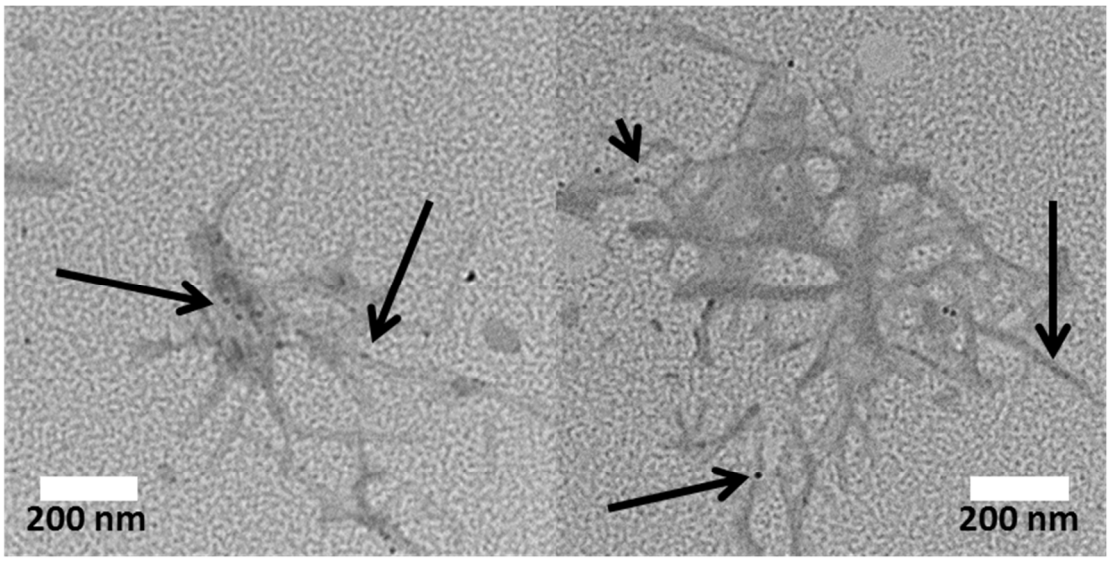

Figure S28: TEM micrographs for PE_{36}-*b*-$PBocAmOx_{15}$-*b*-P*i*$PrOx_{145}$ after 24 hours at 65 °C in water (0.33 mg mL^{-1}) and *in-situ* reduced $HAuCl_4$.